



## Adsorption of Rhodamine B From Industrial Wastewater Using Bottom Ash Adsorbent from Palm Oil Mill Boiler Combustion: A Fixed-Bed Column Study

Rizki Rianda<sup>1</sup>, Muhammad Zikri Maulana<sup>1</sup>, Meutia Kurniawan<sup>1</sup>, Muhammad Ishak Idrus  
Panjaitan<sup>1</sup>, Muhammad Yahdi Salim<sup>1</sup>, Novi Sylvia<sup>1</sup>, Zulmiardi<sup>2</sup>, Meriatna<sup>1</sup>, ✉

DOI: <https://doi.org/10.15294/jbat.v13i2.10702>

<sup>1</sup>Department of Chemical Engineering, Faculty of Engineering, University of Malikussaleh, Jl. Batam, Blang Pulo, Kec. Muara Satu, Kota Lhokseumawe, Provinsi Aceh, Indonesia

<sup>2</sup>Department of Mechanical Engineering, Faculty of Engineering, University of Malikussaleh, Jl. Batam, Blang Pulo, Kec. Muara Satu, Kota Lhokseumawe, Provinsi Aceh, Indonesia

### Article Info

Article history:

Received

29 July 2024

Revised

13 November 2024

Accepted

19 December 2024

Published

December 2024

Keywords:

Adsorbent;

Adsorption;

Bottom Ash;

Fixed-Bed Column;

Rhodamine B.

### Abstract

Increased textile industry production increases water pollution, especially rhodamine B dyes that are difficult to degrade. Global efforts to reduce water pollution through the adsorption process have been carried out with various adsorbents, the utilization of bottom ash from palm oil mill boiler combustion waste is still very minimal. This study examines the effect of contact time and bottom ash adsorbent mass on the adsorption capacity and absorption efficiency of rhodamine B using a fixed bed column adsorption process. The results showed that the longer the adsorption time, the higher the absorption efficiency. In the rhodamine B adsorption process, the best absorption efficiency was 98.308% at 10 cm bed height for 120 minutes and the best absorption capacity was 0.474 mg/g at 12 cm bed height for 150 minutes. The  $R^2$  price of Langmuir isotherm was 0.9999. FTIR analysis showed the presence of -OH, C-H, C=C and C-O functional groups that play a role in the adsorption process. The surface area of bottom ash from SAA test was 94.517 m<sup>2</sup> /g. The SEM-EDX test analysis results had dominant elements of C, O and Si which showed good adsorption activity. From the results of the study that bottom ash from the combustion of oil palm mill boilers can be used as an effective adsorbent in reducing rhodamine B.

### INTRODUCTION

The industrial sector in Indonesia is experiencing rapid development. The textile industry is one of the sectors witnessing an increase in production. According to the (Ministry of Industry., 2024), the growth of the textile industry in the first quarter of 2024 reached 2.64%. This has led to an increase in the amount of waste generated from production processes. The waste produced by the textile industry typically consists of dyes, azo compounds, and their derivatives. If these dyes are discharged into water streams and persist for extended periods, they can contaminate water due to their stable, recalcitrant, colorant, toxic,

mutagenic, and carcinogenic properties (Ariyanto et al., 2021). One of the dyes from textile industry effluents that has garnered attention is Rhodamine B (Furozi et al., 2022)

Rhodamine B (C<sub>28</sub>H<sub>31</sub>ClN<sub>2</sub>O<sub>3</sub>) is a synthetic dye that is polar, highly soluble in water, and resistant to natural degradation by microorganisms (Mading et al., 2024). The permissible concentration of Rhodamine B in water bodies is 5-10 mg/L (Ulya et al., 2022). Excessive presence of Rhodamine B in aquatic environments can damage ecosystems. The dangers of Rhodamine B become more severe when it enters the human body. Rhodamine B is hazardous to health because it contains heavy metals and

**Table 1.** Adsorption capacity of rhodamine b for various adsorbent.

Adsorbent	Mass Adsorbent	Capacity of Adsorption	Reference
Durian Peel	46.74 gr	490.73 mg/g	(Rahman et al., 2022)
Gumitir Plant Stem	1 gr	2.4007 mg/g	(Sahara et al., 2018)
Langsat Peel	0.2 gr	2.099 mg/g	(Bahrizal et al., 2020)
Durian Peel	0.2 gr	18.413 mg/g (pH 4) and 24.64 mg/g (200 rpm)	(Ulya et al., 2022)
White sea bass scales	0.8 gr	0.6298 mg/g	(Latupeirissa et al., 2024)
Oil Palm Fronds	1 gr	9.0490 mg/g	(Sa'bandi et al., 2021)
Spent Coffee Ground	1 gr	0.017 mg/g, 0.047 mg/g, 0.496 mg/g	(Mading et al., 2024)

chlorine compounds that are toxic and carcinogenic, thus increasing the risk of cancer (Bahrizal et al., 2020). Therefore, the dangers of Rhodamine B entering the human body can elevate the risk of various serious diseases (Kurniawan et al., 2020).

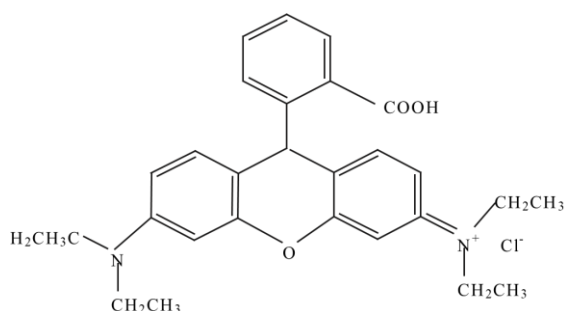


Figure 1. Chemical structure of rhodamine B.

To mitigate the risks associated with Rhodamine B, adsorption is one of the most effective alternatives, as it has no harmful side effects and utilizes simple equipment (Ulya et al., 2022). Adsorption is a physical and chemical process that binds a substance to the surface of another material, whether solid or liquid, in a layered manner. Adsorption occurs between solid and liquid substances, as well as between solid and gaseous substances (Muhammad et al., 2021). Previous studies have investigated Rhodamine B adsorption using various adsorbents to degrade the dye. Research related to adsorption using different types of adsorbents is presented in Table 1. However, the utilization of bottom ash from palm oil mill boiler combustion waste remains minimally explored.

Bottom ash, a by-product of palm oil mill boiler combustion, has significant potential as an adsorbent for removing water pollutants. Bottom ash contains high levels of silica and carbon, making it a promising material for utilization

(Alviana et al., 2021). In addition to its high carbon and silica content, bottom ash also exhibits high porosity and a large surface area, making it suitable for use as an adsorbent (Fatimah et al., 2019). The use of bottom ash as an adsorbent not only provides a sustainable solution for waste management but also offers the potential to address water quality challenges in a cost-effective manner. Its effectiveness, sustainability, and potential applications make it an attractive option for addressing water pollution.

This study aims to examine the effects of contact time and adsorbent mass of bottom ash on the adsorption capacity of Rhodamine B and to analyze the adsorption efficiency of the bottom ash adsorbent.

## MATERIALS AND METHOD

### MATERIALS

Bottom ash used in the study was obtained from PT Syaukath Sejahtera Palm Oil Mill, North Aceh. Rhodamine B ( $C_{28}H_{31}ClN_2O_3$ ) was used as artificial material. The supporting raw materials used were tapioca flour and distilled water as a mixture for making tapioca glue.

### Analysis Method

Fourier Transform Infrared Spectroscopy (FTIR) is a spectroscopic measurement method to detect the molecular structure of compounds, Surface Area Analyzer (SAA) was used to characterize the surface area, pore distribution, and desorption of a material and Scanning Electron Microscopy (SEM) was used to observe finer surface structures and shapes.

### Adsorbent Preparation

Bottom ash from palm oil mill boiler combustion was dried in an oven at  $110^{\circ}C$  to reduce

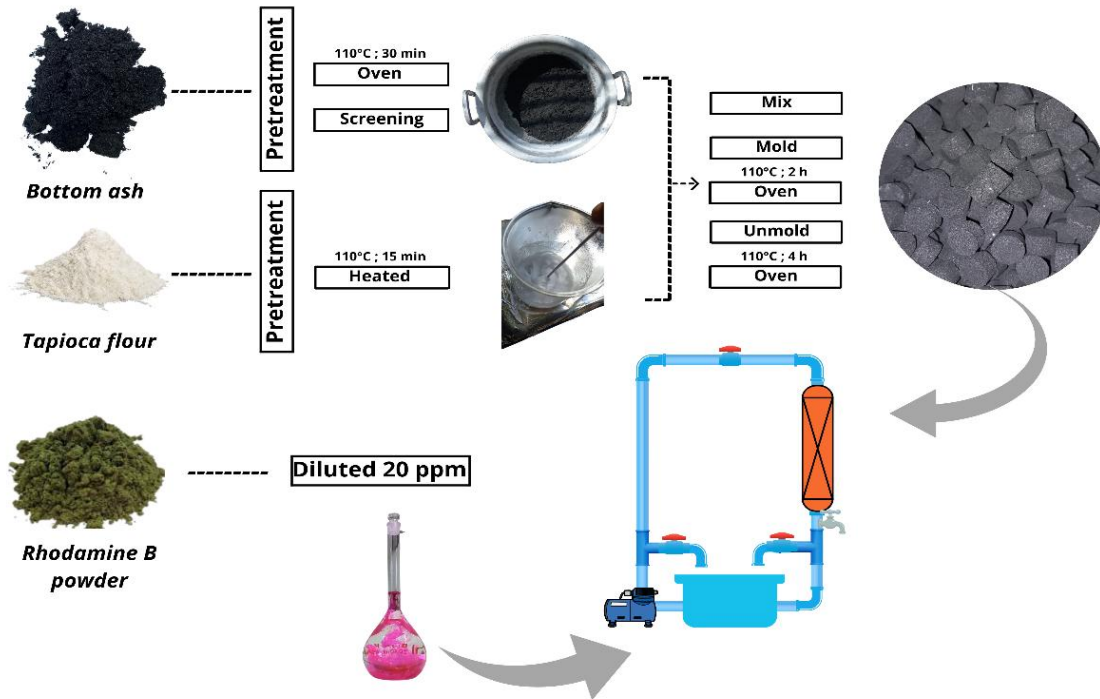


Figure 2. Process diagram of rhodamine B adsorption.

its moisture content, then sieved using a 20-mesh sieve. Fifteen grams of tapioca flour and 45 ml of distilled water were mixed and heated at 110°C to create an adhesive. The sieved bottom ash was thoroughly mixed with the adhesive. This mixture was then molded using adsorbent molds with a diameter of 1.5 cm and a height of 1 cm. The molded adsorbents were dried in an oven for 2 hours at 110°C and then removed from the molds.

**Preparation of Synthetic Rhodamine B Solution**

A 20 mg/L Rhodamine B solution was prepared by dissolving 0.06 grams of Rhodamine B in 1000 ml of distilled water in a 1000 ml volumetric flask and homogenized. This solution was then transferred to the adsorption apparatus container and an additional 2000 ml of distilled water was added and homogenized again.

**Column Adsorption Process**

In the initial stage, the prepared adsorbents were placed in the fixed-bed column at varying bed heights: 6 cm, 8 cm, 10 cm, and 12 cm. The column was then filled with 3000 ml of Rhodamine B solution at a flow rate of 10 L/minute, with contact times varying at 30, 60, 90, 120, and 150 minutes.

The process of Rhodamine B adsorption by bottom ash adsorbent in this experiment is illustrated in Figure 2.

**Testing Phase**

This research was conducted to determine the optimal contact time and adsorbent mass of bottom ash in the adsorption process of Rhodamine B. The testing was performed using a UV-Vis spectrophotometer to obtain results on adsorption efficiency and adsorption capacity of Rhodamine B.

The adsorption efficiency was calculated using Eq. (1):

$$\text{Efficiency} = \frac{C_o - C_e}{C_o} \times 100\% \quad (1)$$

Where  $C_o$  is the initial concentration of the solution (mg/L) and  $C_e$  is the final concentration of the solution (mg/L) (Sylvia, et al., 2021b).

The adsorption capacity was analyzed using the Eq. (2).

$$Q_e = \frac{v}{m} \times (C_o - C_e) \quad (2)$$

Where  $Q_e$  is the adsorption capacity (mg/g),  $V$  is the volume of solution (Liter),  $m$  is the mass of adsorbent used (gram),  $C_o$  and  $C_e$  is the initial concentration of the solution (mg/L) and the final concentration of the solution (mg/L) consecutively (Sylvia, et al., 2021b).

The bottom ash adsorbent from palm oil mill boiler combustion underwent several tests, including functional group testing with Fourier Transform Infrared Spectroscopy (FTIR), surface area testing using Surface Area Analyzer (SAA), and surface morphology, structure, and sample composition testing using Scanning Electron Microscopy (SEM).

The distribution of Rhodamine B molecules at equilibrium in the adsorbent and solution is crucial for determining the maximum adsorption capacity. Several isotherm models can be used to describe the adsorption distribution at equilibrium. The Langmuir isotherm model assumes monolayer adsorption on a homogeneous surface, while the Freundlich isotherm model assumes adsorption occurs on a homogeneous surface with different adsorption energies and occurs on non-identical parts (Setyorini et al., 2023).

Linear form of Langmuir Isotherm is shown in Eq. (3).

$$\frac{C_e}{Q_e} = \frac{1}{Q_m b} + \frac{C_e}{Q_m} \tag{3}$$

Where,  $C_e$  is the final concentration of the solution (mg/L),  $Q_e$  is the adsorption capacity (mg/g),  $Q_m$  is the monolayer adsorption capacity (monolayer) (mg/g) and  $b$  is the constant related to adsorption energy (L/mg) (Setyorini et al., 2023).

The linearized form of Freundlich Isotherm equation is shown in Eq. (4).

$$\log Q_e = \log K_f + \frac{1}{n} \log C_e \tag{4}$$

Where,  $K_f$  is the relative adsorption capacity of the adsorbent (mg/g) and  $1/n$  is the constant indicating the intensity of the adsorption process (Setyorini et al., 2023).

### RESULTS AND DISCUSSION

The results of Rhodamine B adsorption using bottom ash from palm oil mill boiler with UV-Vis spectrophotometer to determine the absorbance value, with a Rhodamine B solution volume of 3000 ml and a flow rate of 10 L/minute, are presented in Table 2. This study varied the bed height, namely 6 cm with 62 grams of adsorbent mass, 8 cm with 80 grams of adsorbent mass, 10 cm with 100 grams of

Table 2. Rhodamine B Adsorption Results Data

Bed Height (cm)	Time (minute)	Concentration (ppm)		Absorbance ( $\lambda = 553 \text{ nm}$ )	Adsorption Efficiency (%)	Adsorption Capacity ( $Q_e$ )
		Initial ( $C_0$ )	Final ( $C_e$ )			
6	30		7.36173	0.13066	63.19136	0.61153
	60		4.51543	0.08455	77.42284	0.74925
	90	20	2.45247	0.05113	87.73765	0.84907
	120		1.07901	0.02888	94.60494	0.91553
	150		0.80123	0.02438	95.99383	0.92897
8	30		6.71358	0.12016	66.43210	0.49824
	60		3.51111	0.06828	82.44444	0.61833
	90	20	1.42284	0.03445	92.88580	0.69664
	120		0.53580	0.02008	97.32099	0.72991
	150		0.62346	0.02150	96.88272	0.72662
10	30		4.06728	0.07729	79.66358	0.47798
	60		1.49568	0.03563	92.52160	0.55513
	90	20	0.86173	0.02536	95.69136	0.57415
	120		0.33827	0.01688	98.30864	0.58985
	150		0.57654	0.02074	97.11728	0.58270
12	30		2.47531	0.05150	87.62346	0.42398
	60		1.28210	0.03217	93.58951	0.45285
	90	20	0.70370	0.02280	96.48148	0.46685
	120		0.55370	0.02037	97.23148	0.47047
	150		0.40494	0.01796	97.97531	0.47407

adsorbent mass, and 12 cm with 124 grams of adsorbent mass.

### Adsorption Efficiency

Adsorption efficiency indicates how effective the adsorbent is in adsorbing the adsorbate. Effective adsorption efficiency can be obtained after analysis using a UV-Vis spectrophotometer. Figure 3 shows the effect of contact time on Rhodamine B adsorption by adsorbents with different bed heights.

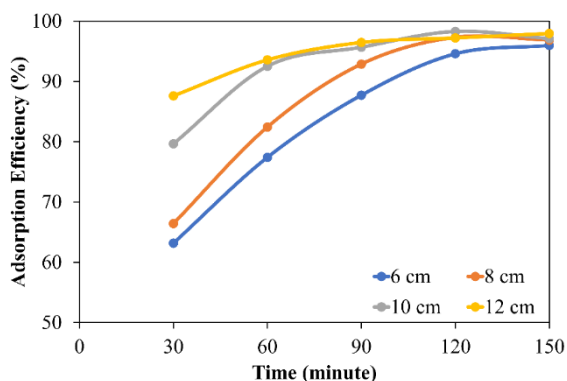


Figure 3. Relationship between time and bed height on adsorption efficiency.

After obtaining the final concentration value, calculations were performed to find the adsorption efficiency. The best adsorption efficiency for 6 cm bed height was obtained at 150 minutes, which is 95.993%. For 8 cm bed height at 120 minutes, it was 97.320%. For 10 cm bed height at 120 minutes, it was 98.308%. For 12 cm bed height at 150 minutes, it was 97.975%. According to (Latupeirissa et al., 2024), the longer the adsorption time, the more adsorbent particles interact with Rhodamine B, thus increasing the adsorption efficiency. Adsorption efficiency is in line with the increase in bed height. According to (Sylvia et al., 2019), the greater the bed height, the greater the adsorption efficiency. This occurs because the amount of adsorbent increases, so the contact area between fluid and adsorbent also increases. However, at 12 cm bed height, there was a decrease in adsorption efficiency caused by saturated adsorbent, where the pores of the adsorbent surface were covered by adsorbate (Latupeirissa et al., 2024).

### Adsorption Capacity

Adsorption capacity indicates the amount of adsorbate that can accumulate on the adsorbent surface. Maximum adsorption capacity can be

obtained after testing the parameters that affect adsorption. The capacity test results can be seen in Figure 4.

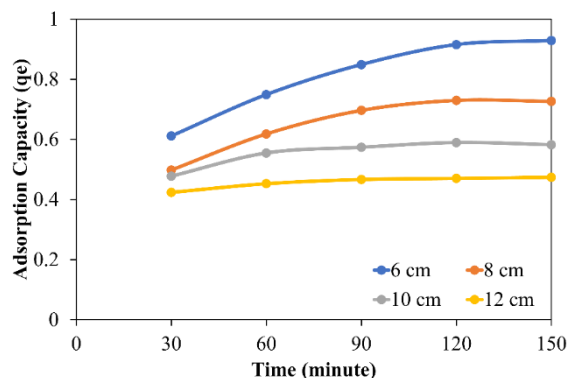


Figure 4. Relationship between time and bed height on adsorption capacity.

Calculations were performed to find the adsorption capacity. The best adsorption capacity for 6 cm bed height was obtained at 150 minutes, which is 0.928 mg/g. For 8 cm bed height at 120 minutes, it was 0.729 mg/g. For 10 cm bed height at 120 minutes, it was 0.589 mg/g. For 12 cm bed height at 150 minutes, it was 0.474 mg/g. Our results are consistent with the theory from previous research, that the larger the bed height, the smaller the adsorption capacity (Meriatna et al., 2021).

### Adsorption Isotherm

Adsorption equilibrium, often studied through the adsorption isotherm approach, is an essential basis for understanding the adsorption process, especially to know how many adsorbate molecules can be adsorbed by porous materials (Sylvia et al., 2021a). The Freundlich and Langmuir adsorption isotherms of Rhodamine B are shown in Table 3.

The adsorption isotherm shows the amount of substance adsorbed per gram of adsorbent at a constant temperature. Determination of adsorption isotherm parameters was conducted using the linear regression method. For the Langmuir isotherm model, the maximum monolayer adsorption capacity ( $Q_m$ ) and Langmuir isotherm constant ( $K_f$ ) can be calculated from the slope and intercept obtained from the plot between  $C_e/Q_e$  and  $C_e$ . For the Freundlich isotherm model, the isotherm constant value ( $K_f$ ) and equilibrium constant value ( $n$ ) can be calculated from the slope and intercept obtained from the plot between  $\log Q_e$  and  $\log C_e$  (Setyorini et al., 2023). From the

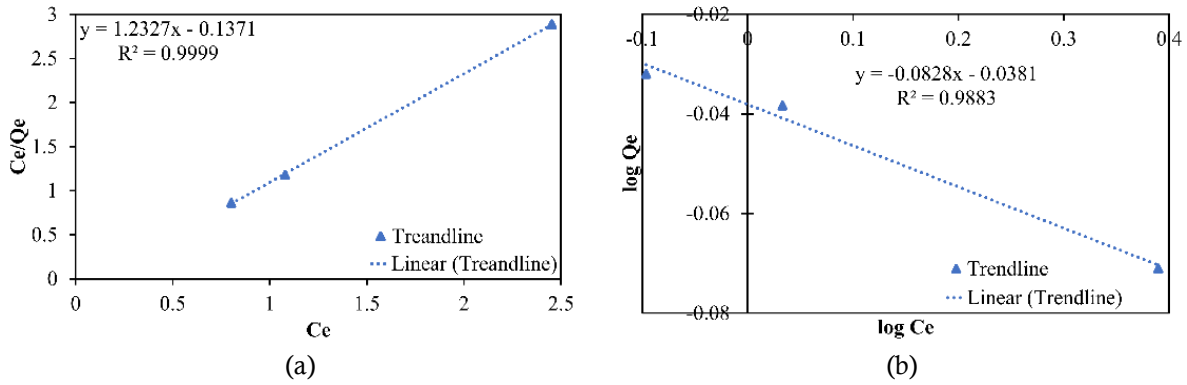


Figure 5. Linear plot for determination of adsorption constants with (a) Langmuir isotherm and (b) Freundlich isotherm models.

Table 3. Langmuir and Freundlich isotherm parameters for rhodamine B adsorption.

Type	Parameter	Unit	Non-Linear Equation
Langmuir			
$Q_m$	-0.8112	mg/g	$Q_e = \frac{Q_m b C_e}{1 + b C_e}$
B	-8.9887	L/mg	
$R^2$	0.9999	-	
Freundlich			
$K_f$	0.9160	mg/g	$Q_e = K_f + C_e^{1/n}$
n	-12.0742	-	
$R^2$	0.9883	-	

research results, the adsorption isotherm tends to align with the Langmuir Isotherm equation.

**Fourier Transform Infrared Spectroscopy Analysis (FTIR)**

FTIR is a spectroscopic measurement method to detect the molecular structure of compounds. In sample measurements using FTIR spectrophotometer instruments, the measurement results obtained are in the form of spectra (Subamia et al., 2023).

FTIR analysis provides important insights into the functional groups involved in the adsorption of Rhodamine B on bottom ash adsorbent. From Figure 6, the FTIR spectrum shows peaks at 3743.83-3763  $cm^{-1}$  indicating the presence of free -OH or non-hydrogen bonded hydroxyl groups. The range of 2914-2981  $cm^{-1}$  indicates the presence of aliphatic methyl (-CH<sub>3</sub>) and methylene (-CH<sub>2</sub>-) groups. The peak at 1901  $cm^{-1}$ , although uncommon, is related to C=C vibrations in conjugated alkene or aromatic systems. The frequency at 1467  $cm^{-1}$  indicates C-H bonding vibrations in methyl or methylene groups, as well as C=C vibrations in aromatic rings. The frequency at 1238  $cm^{-1}$  is related to C-O stretching vibrations in esters, ethers, or phenols. Lastly,

frequencies in the fingerprint region (958  $cm^{-1}$  and 761  $cm^{-1}$ ) are very specific and indicate the presence of out-of-plane C-H bonding vibrations in aromatic systems or aromatic ring vibrations. The interaction between -OH, C-H, C=C, and C-O groups on the adsorbent with Rhodamine B plays a significant role in the adsorption process (Azhagapillai et al., 2021).

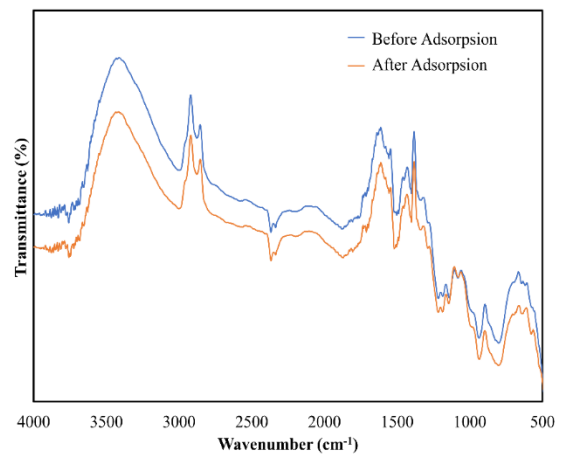


Figure 6. FTIR bottom ash result.

**Surface Area Analyzer (SAA) Test**

Surface Area Analyser (SAA) is a tool used to characterize the surface area, pore distribution,

and desorption of a material (Putri & Ratnawulan., 2019). The SAA characterization test aims to determine the surface area of bottom ash as an adsorbent. The tested sample was conducted by injecting nitrogen into bottom ash at a temperature of 130°C. It was found that the active mass of bottom ash adsorbent powder has a specific surface area of 94.517 m<sup>2</sup>/g. This indicates that bottom ash has a large surface area, thus capable of providing better adsorption capacity (Ali et al., 2020).

### Scanning Electron Microscopy (SEM) Test

SEM (Scanning Electron Microscopy) can observe finer surface structures and shapes, equipped with EDX (Energy Dispersive X-Ray Spectroscopy) which can detect elements in the sample, and also the surface observed through electron conductors (Sylvia et al., 2024). SEM EDX shows dominant elements of C, O, and Si, indicating good adsorption activity. The three types of adsorbent morphological structures were analyzed using SEM with 1000x magnification as shown in Figure 7.

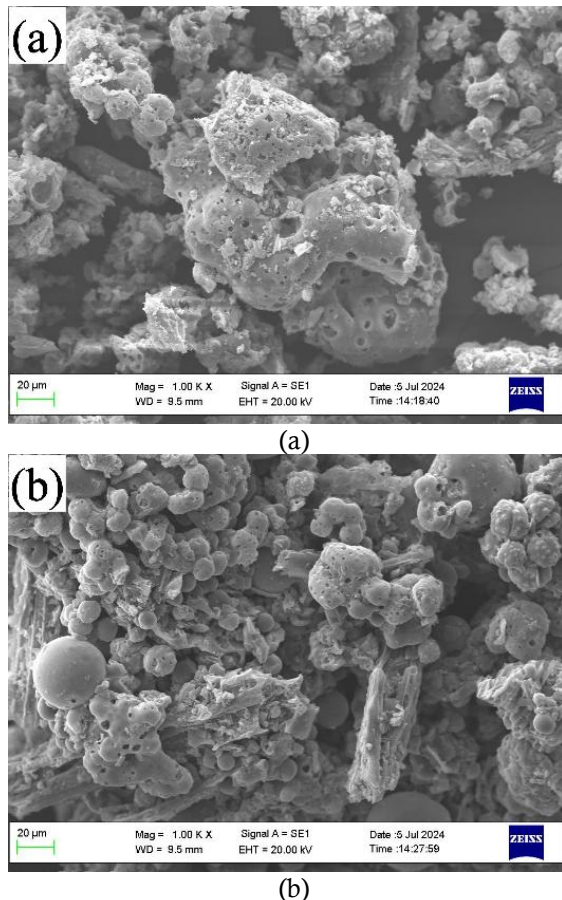


Figure 7. SEM analysis results at 1000x magnification (a) before adsorption, (b) after adsorption.

The SEM analysis results of bottom ash shown in Figure 7 indicate that the adsorbent before adsorption has a more robust adsorbent structure, with agglomeration, cracks, and fractures. Meanwhile, the adsorbent after adsorption has a less robust structure, with agglomeration beginning to erode and break down into smaller clumps, cracks, and fractures, due to the adsorbent starting to melt during the adsorption process (Suryadi et al., 2019).

The EDX analysis results of bottom ash shown in Figures 7 and 8, and Table 4 indicate that the elements C, O, Mg, Si, K, and Ca are components of bottom ash before adsorption, with an average pore size of 9.5 mm. After adsorption, elements C, O, Mg, Al, Si, K, Ca, and Fe were found with an average pore size of 9.6 mm. The highest components before and after adsorption are C, O, and Si, which identify that bottom ash has silica oxide (SiO<sub>2</sub>) as the constituent component of the adsorbent. The EDX analysis results are consistent with the XRD results characteristics and show the same constituent elements. SiO<sub>2</sub> is proven to have good activity in the adsorption process (Sylvia et al., 2021a).

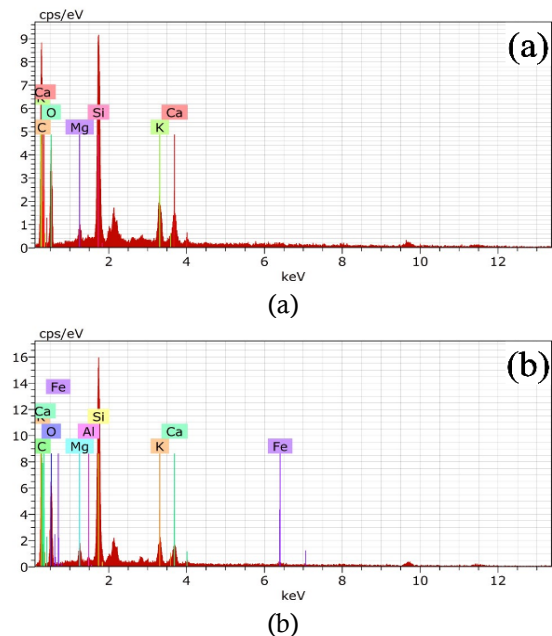


Figure 8. Graph of EDX analysis results (a) before adsorption, (b) after adsorption.

### CONCLUSION

Based on the research conducted, several conclusions can be drawn. In the Rhodamine B adsorption process, the best adsorption efficiency

Table 4. EDX Analysis Results of Adsorbent Before and After Adsorption

Atom (%)	Element							
	C	O	Mg	Al	Si	K	Ca	Fe
Before Adsorption	58.02	32.6	0.87	-	5.54	1.58	1.39	-
After Adsorption	52.13	36.41	0.85	0.13	7.75	1.28	1.29	0.16

was 98.308% at a bed height of 10 cm at 120 minutes, and the best adsorption capacity was 0.474 mg/g at a bed height of 12 cm at 150 minutes. The Langmuir Isotherm has an  $R^2$  value of 0.9999. The interaction between -OH, C-H, C=C, and C-O groups on the adsorbent with Rhodamine B plays a significant role in the adsorption process. The SAA test results show that the active mass of bottom ash adsorbent powder is 94.517 m<sup>2</sup>/g. SEM EDX analysis shows dominant elements of C, Si, and O, with values before adsorption of 5.54 and 32.6, and after adsorption of 7.75 and 36.41, respectively.

#### ACKNOWLEDGMENTS

Acknowledgments are given to the Directorate General of Higher Education Research Technology through the Directorate of Learning and Student Affairs (Belmawa), Malikussaleh University which has funded this research, and the Department of Chemical Engineering, Malikussaleh University which has provided laboratory facilities.

#### REFERENCES

- Ali, M. E., Hoque, M. E., Hossain, S. K. S., Biswas, M.C. 2020. Nanoadsorbents for Wastewater Treatment: Next Generation Biotechnological Solution, *International Journal of Environmental Science and Technology*. Springer Berlin Heidelberg.
- Alviana, A. D., Habsya, C., Agustin, R. S. 2021. Utilization of Rice Husk Ash and Fly Ash as Partial Substitution of Cement in Column Segments of Eco-friendly Concrete Modular Structures. *Indonesian Journal of Civil Engineering Education*. 7(2): 28–36.
- Ariyanto, E., Lestari, D. D., Kharismadewi, D. 2021. Analysis of Adsorption Capacity and Kinetics of Activated Carbon from Ketapang Shells Against Methyl Orange Dye. *Jurnal Dinamika Penelitian Industri*. 32(2): 166–178.
- Azhagapillai, P., Al Shoaibi, A., Chandrasekar, S. 2021. Surface Functionalization Methodologies on Activated Carbons and Their Benzene Adsorption. *Carbon Letters*. 31(3): 419–426.
- Bahrizal, Adella, F., Kurniawati, D. 2020. Adsorption of Rhodamine B from Aqueous Solution Using Langsat (*Lansium domesticum*) Shell Powder. *Advances in Biological Sciences Research*. 10 (ICoBioSE 2019): 273–276.
- Fatimah, Tarigan, B. P., Ramadhan, A. 2019. Activation of Bottom Ash from Coal Combustion to Reduce Phosphate Compound Content in Water. *Jurnal Teknik Kimia USU*. 8(2): 72–78.
- Furozi, N., Fajriyati, I., Artsanti, P., Krisdiyanto, D. 2022. Adsorption of Rhodamine B and Congo Red Dyes with Silica Gel from Sugarcane Bagasse Waste (*Saccharum officinarum*). *Indonesian Journal of Materials Chemistry*. 3(2): 53–59.
- Kurniawan, M. A., Damayanti, T., Ramadhanty, B., Iynayah, C., Purwiandono, G. 2020. Use of Ketapang Seeds for Biofuel Production as Renewable Energy Using Catalytic Hydrocracking Method. *AIP Conference Proceedings*. 2229(April): 1–6.
- Latupeirissa, J., Fransina, E. G., Tanasale, M. F. J. D. P. 2024. Adsorption Isotherm of Rhodamine B Using Activated Carbon of White Snapper (*Lates calcarifer*) Scale Waste as Adsorbent. *Fullerene Journal of Chemistry*. 9(1): 26–33.
- Mading, R., Batu, M. S., Kolo, M. M., Saka, A.R. 2024. Preparation of Activated Carbon from Lontar Fruit Shell (*Borassus flabellifer* L.) as Rhodamine B Adsorbent. *Molluca Journal of Chemistry Education*. 14(1): 10–21.
- Meriatna, Afriani, R., Maulinda, L., Suryati, Zulmiardi. 2021. Optimization of Pb<sup>2+</sup> Ion Adsorption Using Rice Husk Activated Carbon in Fixed Bed Column with RSM (Response Surface Methodology)



- Approach. *Jurnal Teknologi Kimia Unimal*. 10(1): 100.
- Ministry of Industry. 2024. Textile, Apparel, and Footwear Industries Becoming More Expansive in the First Quarter of 2024. Available online at: <https://bpt.kemendag.go.id/blog/industri-teksstil-pakaian-jadi-dan-alas-kaki-makin-ekspansif-di-triwulan-pertama-2024>. Accessed on 15 July 2024.
- Muhammad, Meriatna, Afriani, N., Mulyawan, R. 2021. Oyster Shell Waste (*Crassostrea Gigas*) as a Cheap Adsorbent for Adsorption of Methylene Blue Dyes: Equilibrium and Kinetics Studies. *International Journal of Engineering, Science and Information Technology*. 1(4): 95–102.
- Putri, A. Z., Ratnawulan. 2019. Theoretical Analysis of Zirconium Dioxide (ZrO<sub>2</sub>) Nanoparticles. *Pillar of Physics*. 12(1): 70–76.
- Rahman, T., Muis, L., Suryadri, H. 2022. Effect of Bed Weight on Efficiency and Adsorption Capacity of Rhodamine B Dye with Continuous System. *Jurnal Engineering*. 4(1): 32–38.
- Sa'bandi, F., Aini, S., Nizar, U. K., Khair, M. 2021. Preparation of Activated Carbon from Oil Palm Frond Waste with Ultrasonic Activation as Rhodamine B Adsorbent. *Chemistry Journal of Universitas Negeri Padang*. 10(2): 59–63.
- Sahara, E., Gayatri, S., Suarya, P. 2018. Adsorption of Rhodamine-B Dye in Solution by Activated Charcoal from Gunitir Plant Stems Activated with Phosphoric Acid. *Cakra Kimia Indonesian E-Journal of Applied Chemistry*. 6(1): 37–45.
- Setyorini, D., Arninda, A., Syafaatullah, A. Q., Panjaitan, R. 2023. Determination of Freundlich Isotherm Constant and Adsorption Kinetics of Activated Carbon on Acetic Acid. *Eksergi*. 20(3): 149.
- Subamia, I. D. P., Widiasih, N. N., Wahyuni, I. G. A. N. S., Kristiyanti, P. L. P. 2023. Optimization of Fourier Transform Infrared (FTIR) Instrument Performance Through Comparative Study of Sample-KBr Composition and Thickness. *Jurnal Pengelolaan Laboratorium Pendidikan*. 5(2): 58–69.
- Suryadi, H., Muis, L., Lingga, R. 2019. Characteristics of Durian Peel Adsorbent Without Modification and Modified with Latex Coating for Rhodamine B Application. *Jurnal Engineering*. 1(2): 30–37.
- Sylvia, N., Dewi, R., Ishak, Janni, M., Putri, M. A. 2024. Utilization of Fly Ash Palm Oil Mill Waste as an Adsorbent of Methylene Blue in a Fixed Bed Column System by Using Response Surface Methodology. *Jurnal Bahan Alam Terbarukan*. 13(2): 28–37.
- Sylvia, N., Fitriani, F., Dewi, R., Mulyawan, R., Muslim, A., Husin, H., Yunardi, Y., Reza, M. 2021a. Characterization of Bottom Ash Waste Adsorbent from Palm Oil Plant Boiler Burning Process to Adsorb Carbon Dioxide in a Fixed Bed Column. *Indonesian Journal of Chemistry*. 21(6): 1454–1462.
- Sylvia, N., Sobrina, L., Nasrun. 2019. Optimization of CO<sub>2</sub> Absorption Process with Activated Carbon Adsorbent Using Computational Fluid Dynamics (CFD) and Response Surface Methodology (RSM). *Jurnal Teknologi Kimia Unimal*. 8(1): 69.
- Sylvia, N., Wijaya, Y. A., Masrullita, Safriwardy, F. 2021b. Effectiveness of Cassava Peel Activated Carbon (*Manihot Esculenta Crantz*) on the Adsorption of Fe<sup>2+</sup> Metal Ions with NaOH Activator. *Jurnal Teknologi Kimia Unimal*. 10(2): 83–91.
- Ulya, A., Nasra, E., Amran, A., Kurniawati, D. 2022. Adsorption of Rhodamine B Dye with Activated Carbon from Durian Peel as Adsorbent. *Jurnal Periodic Jurusan Kimia UNP*. 11(2): 74.